



# **The University of Wisconsin Contribution to the BCC Ion Correlation Experiment on Molybdenum**

**H.V. Smith, Jr., K.Y. Liou, G.L. Kulcinski, and P. Wilkes**

**October 1976**

**UWFDM-177**

***FUSION TECHNOLOGY INSTITUTE  
UNIVERSITY OF WISCONSIN  
MADISON WISCONSIN***

**The University of Wisconsin Contribution to  
the BCC Ion Correlation Experiment on  
Molybdenum**

H.V. Smith, Jr., K.Y. Liou, G.L. Kulcinski, and P.  
Wilkes

Fusion Technology Institute  
University of Wisconsin  
1500 Engineering Drive  
Madison, WI 53706

<http://fti.neep.wisc.edu>

October 1976

UWFDM-177

The University of Wisconsin Contribution to the BCC Ion  
Correlation Experiment on Molybdenum

H. V. Smith, Jr.

K. Y. Liou

G. L. Kulcinski

P. Wilkes

October 1976

UWFD-177

Fusion Technology Program  
Nuclear Engineering Department  
University of Wisconsin  
Madison, Wisconsin 53706

## Table of Contents

I. Introduction . . . . .	1
II. Experimental Procedure . . . . .	1
A. Irradiation Procedure . . . . .	1
B. Transmission Electron Microscopy Procedure . . . . .	6
C. Electron Micrograph Analysis Procedure . . . . .	9
III. Results . . . . .	9
A. University of Wisconsin Irradiated Samples. . . . .	10
B. TEM Measurement on the Common Specimen . . . . .	20
C. Measurement of Void Parameters in the Common Micrograph . . . . .	21
D. Comparison with Other ICE Ion Simulation Results . . . . .	21
IV. Conclusions . . . . .	22
Acknowledgements . . . . .	23
References . . . . .	24

## I. Introduction

This report contains a description of the University of Wisconsin (UW) contribution to the BCC Ion Correlation Experiment on Molybdenum.\* The experiment was initiated by ERDA primarily to check the reproducibility of the data obtained on a reference material by several labs using the heavy ion simulation technique. The BCC Ion Correlation Experiment consisted of three parts: (1) irradiation, TEM examination, and subsequent analysis of annealed Molybdenum specimens supplied by Pacific Northwest Laboratory (PNL), (2) TEM examination and subsequent analysis of a Molybdenum sample irradiated and prepared for microscope examination by the Naval Research Laboratory (NRL), and (3) analysis of an electron micrograph supplied by NRL.

## II. Experimental Procedure

The apparatus and techniques used for the UW contribution to each of the three parts of the BCC Ion Correlation Experiment are described below.

### A. Irradiation Procedure

Table I contains a chemical analysis of the Molybdenum supplied to each of the participating laboratories by PNL. The material supplied to UW was in strip form 7 cm x 1.25 cm x 0.15 mm thick. To accomodate this material into the UW sample holder (Figure I), two 3.2 mm diameter and five 4.8 mm diameter holes were spark machined in the sample strips. The strips were also spark machined in half (making two 3.5 cm x 1.25 cm x 0.15 mm thick strips). This was done to facilitate the subsequent preparation of specimens for TEM examination. After the spark machining process but prior to irradiation, the specimen strips were electropolished in a 15%  $H_2SO_4$ , 85% methyl alcohol solution at

\*The participating labs were Atomics International, Argonne National Laboratory, MIT, Naval Research Laboratory, Oak Ridge National Laboratory, Pacific Northwest Laboratory, U. of Cincinnati, and U. of Wisconsin.

Table I. Material Chemistry for the BCC Ion Correlation Experiment on Molybdenum

- A. Chemical analysis of base material
  - <80 appm carbon, <60 appm oxygen,
  - <0.001 weight % all others
- B. Chemical analysis after pre-irradiation treatment
  - None.
- C. Chemical analysis after ion bombardment
  - C-1. Analysis of entire specimen
    - None.
  - C-2. Analysis of damage zone
    - None.

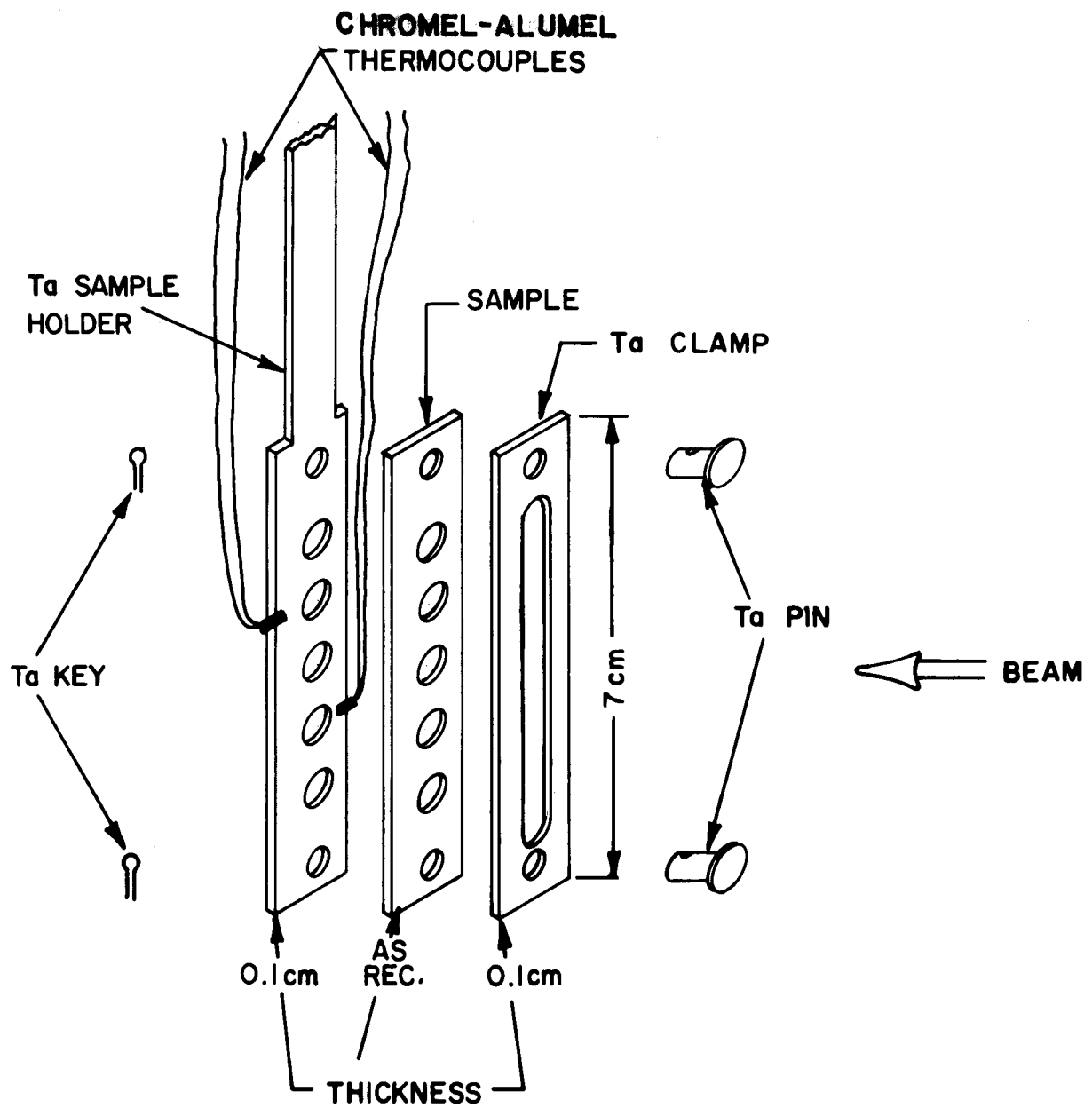


Figure 1. Detail of the sample holder assembly.

-20°C and 10 volts to give a smooth surface. Table II summarizes the pre-treatment of the specimens.

The specimens were irradiated using the U. W. tandem Van de Graaff accelerator as described elsewhere.<sup>(1)</sup> Briefly, the specimens were bombarded with ~25 particle nA of either 17.0 or 18.8 MeV Cu<sup>4+</sup> ions. The charge state of the Cu beam was determined by elastic scattering of the beam off of a thin gold foil.<sup>(1)</sup> The energy E of the beam is given by  $E = (q + 1)V$ , where q is the charge state of the beam and V is the accelerator dome voltage (measured with a generating voltmeter).

The samples were irradiated in three separate groups. The first group contained six specimens of which two were irradiated at 1000°C, two at 900°C, and two at 800°C to damage levels near 1 dpa (approximately 1  $\mu$ m from the surface). These irradiations were carried out at pressures near  $1 \times 10^{-8}$  Torr. The specimens were irradiated from highest to lowest temperature in order to minimize post-irradiation annealing effects. The second group also contained six specimens of which one was irradiated at 1000°C, two at 900°C and two at 800°C to a damage level near 2 dpa. The sixth specimen in this group was irradiated at 700°C to ~1 dpa. The pressure during irradiation of these specimens was near  $5 \times 10^{-9}$  Torr. The last group contained only one specimen. It was irradiated at 900°C to 19 dpa at a pressure near  $1 \times 10^{-8}$  Torr. Partial pressure analysis prior to the first 1000°C run revealed that the residual gas in the sample chamber was composed of 57% H<sub>2</sub>, 18% CO, 22% H<sub>2</sub>O, 2% CO<sub>2</sub>, and 1% CH<sub>4</sub>.

The particle flux for all but the 19 dpa specimen was determined by periodically measuring the beam current striking an insertable faraday cup. Knowledge of the charge state of the beam allows the beam particle current to be calculated. The total fluence was then calculated from knowledge of the irradiation time (about 2 hours for the 2 dpa specimens). The current striking the 19 dpa specimen was



Table II. Pre-Treatment of BCC Ion Correlation Experiment Molybdenum Specimens

- A. Electropolishing (solution, temperature, surface removal, etc.)  
Polished in 15%  $H_2SO_4$ , 85% methyl alcohol at  $-20^{\circ}C$  and 10 V  
to smooth surface after strip preparation in B.
- B. Other preparation (mechanical polish, chemical etch, etc.)  
Spark machined seven holes in strips, then spark machined strips  
in half followed by polish in A.
- C. Surface smoothness  
Generally very smooth, with some preferential grain attack.

measured directly and integrated to obtain the fluence. The displacement damage vs depth curve as well as the position of the deposited copper ions is shown in Figure II. The dpa values were calculated with the E-DEP-1 code<sup>(2)</sup> assuming  $E_d = 61.7$  eV, an efficiency of 0.8, and an atom density of  $6.42 \times 10^{22}$  per  $\text{cm}^3$ . The dpa rate at the region of analysis ( $\sim 1 \mu\text{m}$  from the sample surface, see below) is  $\sim 4 \times 10^{-4}$  dpa/sec.

In order to minimize the effects of the sample surface and the deposited Cu ions, TEM analysis of the damage was done  $\sim 1 \mu\text{m}$  from the sample surface (Figure II). This analysis zone is  $>1 \mu\text{m}$  from the deposited Cu atoms. A diffusion calculation shows that for the 2 dpa specimens the deposited Cu atoms move  $<0.2 \mu\text{m}$  and for the 19 dpa specimen  $<0.6 \mu\text{m}$  from their initial position during the course of the irradiation. Therefore, impurity effects due to the use of a copper beam may not be a problem.\* The ability to do the TEM analysis away from both the surface and the stopped ions is one of the advantages of using 17-19 MeV as opposed to 2-5 MeV heavy ion beams. Table III contains a summary of the irradiation parameters for each of the six irradiated samples which were successfully analyzed on the electron microscope.

After irradiation, the same electropolishing conditions used in the pre-irradiation polish were used to remove  $\sim 1 \mu\text{m}$  from the irradiated surface. The amount of surface removed was determined to within  $\pm 0.1 \mu\text{m}$  by optical interference microscopy. The 3mm diameter TEM specimens were then cut from the sample strip and back thinned to perforation in a Fischione jet electropolisher with the same polishing solution but at  $-50^\circ\text{C}$  and 70 V.

#### B. Transmission Electron Microscopy Procedure

The specimens were examined in a Jeolco 100B electron microscope operated at 120 kV voltage. Voids were imaged under weak diffraction conditions at high magnification and focused as precisely as possible to minimize the surrounding dark fringes for void size measurement. The magnification

---

\* A small amount of precipitation was observed in the 19 dpa specimen as discussed in section IIIC.

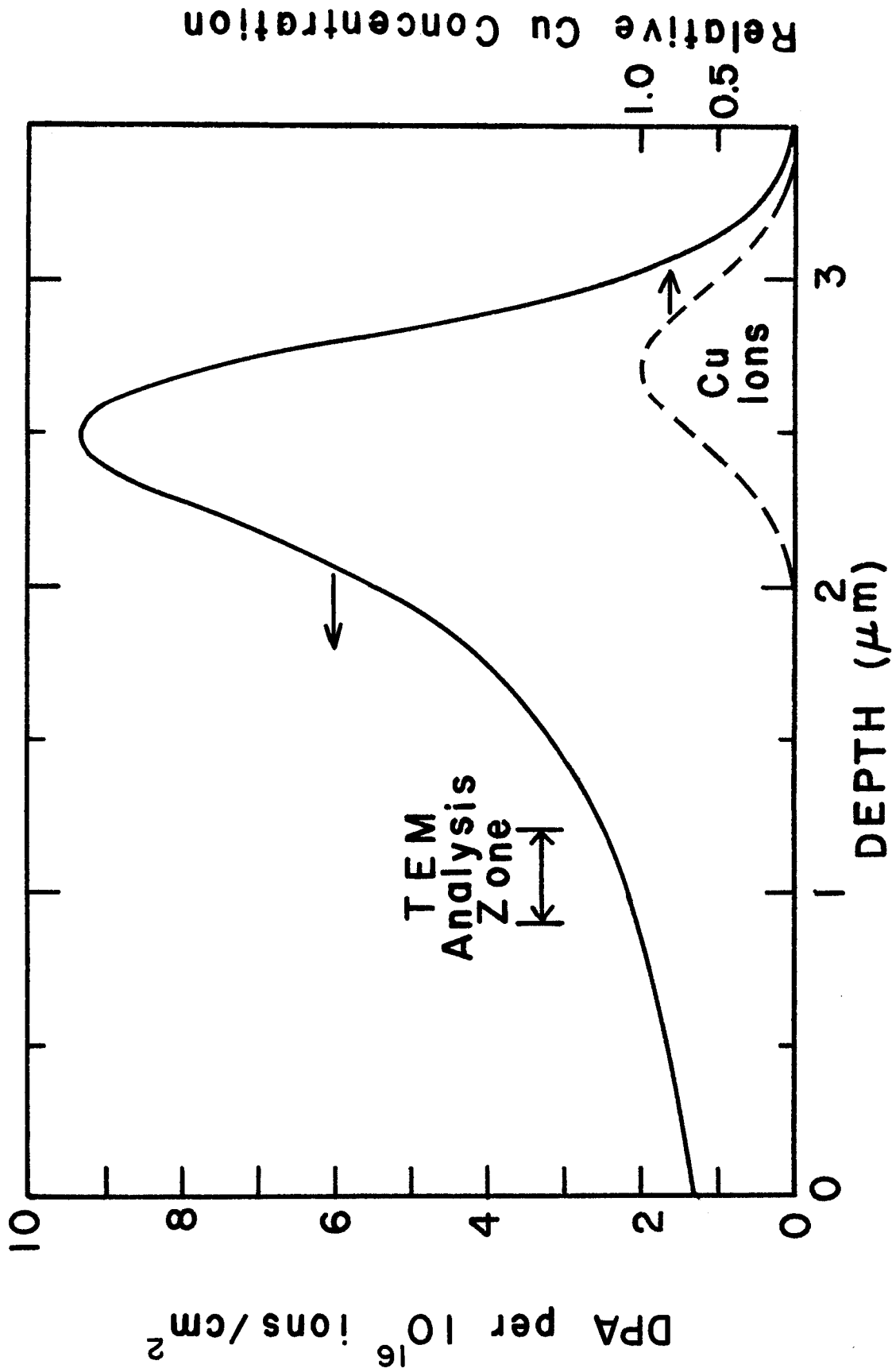


Figure II. Damage curve for 17 MeV Cu on Molybdenum calculated using the E-DEP-1 code of ref. (2). Also indicated on the figure are the TEM analysis zone and the location of the deposited copper ions.

Table III. Irradiation Parameters

A. Specimen Environment

Spec. Ident.	Temp (°C)	Temp. Variation (°C)	Time (pre-irrad)	Time (irrad)	Time at Temp. (post-irrad)	Vac. (Torr)	Vacuum (Torr) (low to high value)
2	1000	$\pm 3$	Annealed by PNL at 1600°C for 2 hours near $10^{-6}$ Torr.	47 min (Beam on 39, off 8)	140 min at 900°C 160 min at 800°C	$2.5 \times 10^{-8}$	$2.2 \times 10^{-8}$ to $2.8 \times 10^{-8}$
3	900	$\pm 4$		112 min (Beam on 30, off 82)	55 min at 900°C 160 min at 800°C	$9.2 \times 10^{-9}$	$8.1 \times 10^{-9}$ to $1.0 \times 10^{-8}$
9	900	$\pm 2$		85 min (Beam on 84, off 1)	325 min at 800°C 50 min at 700°C	$4.9 \times 10^{-9}$	$4.6 \times 10^{-9}$ to $5.2 \times 10^{-9}$
10	800	$\pm 5$		195 min (Beam on 113, off 82)	120 min at 800°C 50 min at 700°C	$4.3 \times 10^{-9}$	$3.8 \times 10^{-9}$ to $4.7 \times 10^{-9}$
12	700	$\pm 10$		40 min (Beam on 29, off 11)	Cooled immediately after irradiation	$4.4 \times 10^{-9}$	$3.8 \times 10^{-9}$ to $4.8 \times 10^{-9}$
13	900	$\pm 10$	↓	1691 min (Beam on 1118, off 573)	145 min at 625°C 80 min at 575°C 65 min at 525°C	$1.4 \times 10^{-8}$	$6.0 \times 10^{-9}$ to $7.0 \times 10^{-8}$

Gas Analysis of Vacuum 57% H<sub>2</sub>, 18% CO, 22% H<sub>2</sub>O, 2% CO<sub>2</sub>, 1% CH<sub>4</sub> at 1000°C.

B. Beam Variables (17-19 MeV Cu<sup>4+</sup> ions)

Spec. Ident.	Highest Current (particle nA)	Lowest Current (particle nA)	Average Current (particle nA)	Integrated Fluence (particle nA-hr) (ions)		Beam Uniformity (%)
2	32	19	31	18	$4.1 \times 10^{14}$	$\pm 20$
3	40	23	32	16	$3.6 \times 10^{14}$	↓
9	27	12	21	30	$6.7 \times 10^{14}$	
10	23	8	17	32	$7.1 \times 10^{14}$	
12	38	9	29	14	$3.2 \times 10^{14}$	
13	18	6	13	234	$5.3 \times 10^{15}$	↓

of the electron microscope was determined to be accurate to within  $\pm 5\%$ . Dislocations and loops were imaged under <sup>a</sup>two beam condition in typical areas to get the average densities. Photographs of interesting grain boundary areas or any unusual features were also taken.

The foil thickness was determined by the stereo pair technique. The average tilt angle was about 9 degrees from the zero degree horizontal position. The accuracy of the tilt angle is about  $\pm 10$  minutes. Foil thicknesses ranged from  $\sim 500 \text{ \AA}$  near the edge of the foil to a maximum of  $2400 \text{ \AA}$ . Photographs of stereo pairs were not taken for the  $800^\circ\text{C}, 2.2 \text{ dpa}$  and  $700^\circ\text{C}, 1.0 \text{ dpa}$  specimens because the images of the small voids and the background contrast were too variable when the specimens were tilted. The thicknesses of these two foils were estimated by the degree of transparency using the observed thickness range from  $500 \text{ \AA}$  to  $\sim 2500 \text{ \AA}$  in other specimens. The accuracy of the foil thickness obtained from the stereo pairs is  $\pm 15\%$  while the uncertainty of the thickness obtained from the transparency measurements is estimated to be  $\pm 50\%$ .

### C. Electron Micrograph Analysis Procedure

The average void diameters and void size distributions were measured with a Zeiss particle size analyzer. For the  $1000^\circ\text{C}, 1.3 \text{ dpa}$  specimen, edges of the cubic voids in <sup>the</sup>(100) foil orientation were measured. For specimens irradiated at <sup>the</sup>900, 800 and  $700^\circ\text{C}$ , <sup>the</sup>diameters were measured assuming spherical void morphology and using the center of the dark fringe surrounding the void. Because the edge of the voids on the surface were polished by the solution, voids intersecting the surface were not counted. A corrected foil thickness of  $t - \bar{d}$  was used to determine the void density, where  $\bar{d}$  is the average void diameter.

### III. Results

We will discuss the results of our irradiations, the NRL TEM sample, and the common micrograph separately.

### A. University of Wisconsin Irradiated Samples

We examined six samples irradiated in the temperature range 700°C-1000°C as discussed in section II-A. Voids were found in each of these specimens and in general were homogeneously distributed. Dislocation loops were observed only in the specimens irradiated to ~2 dpa at 700°C and 800°C and in the specimen irradiated to 19 dpa at 900°C.

The voids in the specimen irradiated at 1000°C were cubes of {100} faces with {110} facets as shown in the micrograph in Figure IIIa. The voids became more spherical as the irradiation temperature decreased. The average void size varied from ~45 Å at lower temperatures to ~250 Å at 1000°C. The volume swelling value at 1000°C included a correction for the observed truncations. Swelling values at all other temperatures were calculated by  $\Delta V/V = \frac{\pi}{6} \rho_v \langle d^3 \rangle_{\text{avg}}$ .

A summary of the damage microstructure observed in the examined specimen is contained in Table IV. The uncertainties given in Table IV are arrived at in the following manner: surface removal, the uncertainty in the interference microscopy determination <sup>is</sup>  $\pm 0.1 \mu\text{m}$ ; dpa value,  $\pm 21\%$  due to  $\pm 20\%$  beam profile non-uniformity<sup>(1)</sup> and  $\pm 5\%$  due to the uncertainty in the surface thickness removal (added in quadrature); mean void size  $\pm 5\%$  due to the uncertainty in the measurement of the microscope magnification; void density  $\pm 25\%$  due to  $\pm 15\%$  uncertainty in foil thickness and  $\pm 5\%$  in the microscope calibration (added twice) except for specimens 10 and 12 where this error is  $\pm 60\%$  due to  $\pm 50\%$  uncertainty in foil thickness plus  $\pm 5\%$  in the microscope calibration; and void volume fraction,  $\pm 20\%$  due to the  $\pm 15\%$  uncertainty in the foil thickness and  $\pm 5\%$  in the microscopic calibration (added only once due to cancelation in the  $\rho_v \langle d^3 \rangle_{\text{avg}}$  product) except for specimens 10 and 12 where this error is  $\pm 55\%$  due to  $\pm 50\%$  uncertainty in the foil thickness and  $\pm 5\%$  in the microscope calibration. Electron micrographs showing typical

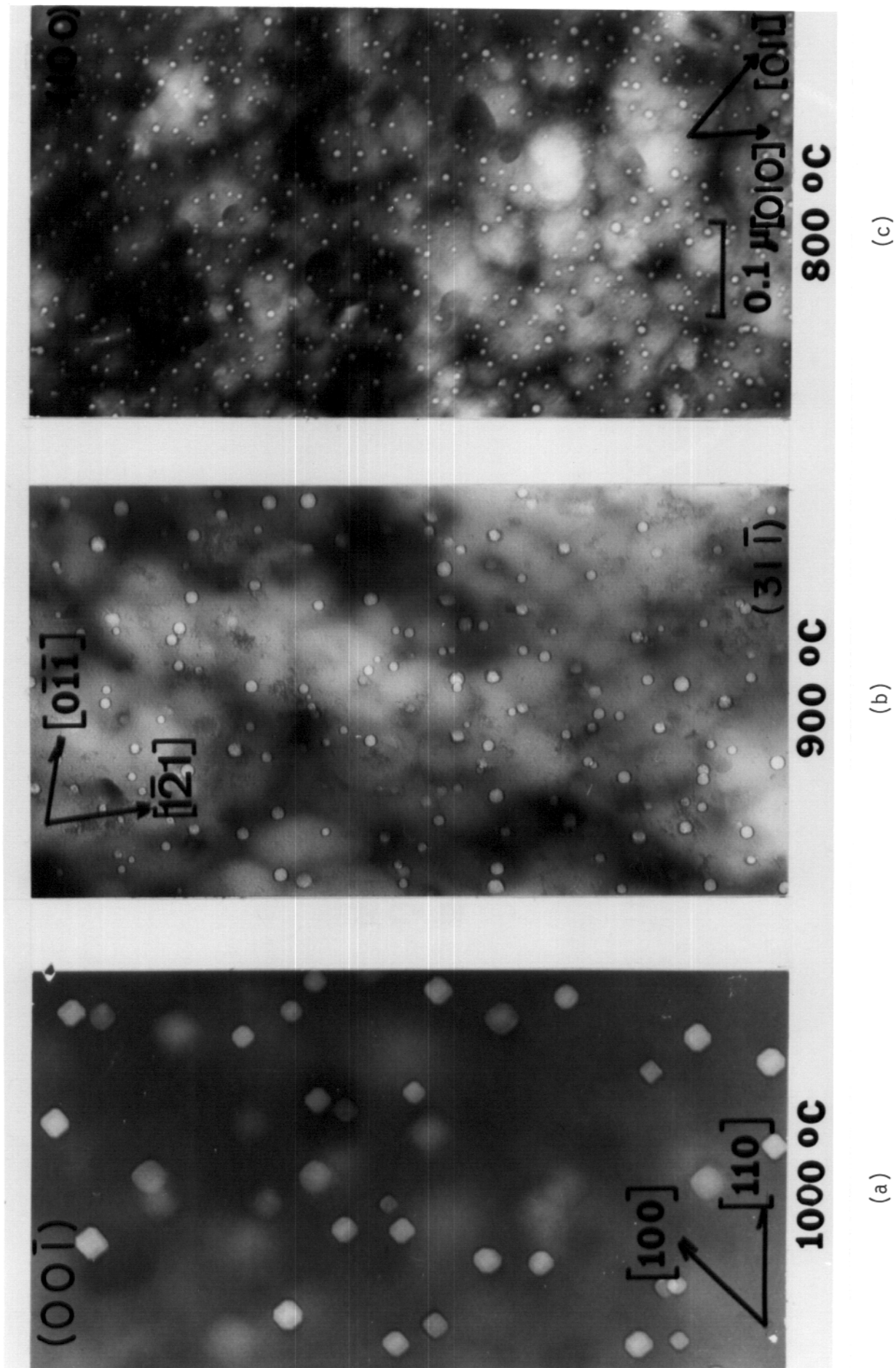


Figure III. Typical microstructure in Mo irradiated with 17-19 MeV copper ions. (a) 1.3 dpa at 1000°C. (b) 1.9 dpa at 900°C. (c) 2.2 dpa at 800°C.

Table IV. Damage Microstructure in the Irradiated Specimens

Specimen No.	Irradiation Temp. (°C)	Calc. dpa (%)	Surface Rem. (µm) ± Error	Mean Void Size (Å)	Total No. of Voids Sized	No. of areas Sampled	Void Density (cm <sup>-3</sup> )	Areas Sampled	Void Volume Fraction (%)	Estimated Error (± %)	Mean Loop Dia. (Angstroms)	Stand. Dev. (Å)	Total No. of Loops Detected	No. of Areas Sampled	Loop Density (cm <sup>-3</sup> )	Line Density (cm <sup>-2</sup> )	Total Distoc. Density * (cm <sup>-2</sup> )
2	1000	1.3 +0.3	0.9 +0.1	252	354	2	5.8 <sub>14</sub> x10 <sup>14</sup>	1	0.76	0.15	-	-	No Loops Detected	-	1x10 <sup>9</sup>	1x10 <sup>9</sup>	1x10 <sup>9</sup>
3	900	1.0 +0.2	0.9 +0.1	78	393	2	6.0 <sub>15</sub> x10 <sup>15</sup>	1	0.17	0.03	-	-	No Loops Detected	-	ND	ND	ND
9	900	1.9 +0.4	0.9 +0.1	98	230	1	6.6 <sub>15</sub> x10 <sup>15</sup>	1	0.39	0.08	-	-	No Loops Detected	-	5x10 <sup>9</sup>	5x10 <sup>9</sup>	5x10 <sup>9</sup>
10	800	2.2 +0.5	1.0 +0.1	44	340	1	1.7 <sub>16</sub> x10 <sup>16</sup>	1	0.11	0.06	160	65	6	2	2x10 <sup>13</sup>	8x10 <sup>8</sup>	9x10 <sup>8</sup>
12	700	1.0 +0.2	1.1 +0.1	48	259	1	1.0 <sub>16</sub> x10 <sup>16</sup>	1	0.08	0.04	76	27	72	1	2x10 <sup>15</sup>	4x10 <sup>9</sup>	9x10 <sup>9</sup>
13	900	1.9 +4	1.2 +0.1	75	1305	2	3.0 <sub>16</sub> x10 <sup>16</sup>	1	0.87	0.17	420	60	4	2	7x10 <sup>12</sup>	1x10 <sup>9</sup>	1x10 <sup>9</sup>

ND - Not Determined

\* Loop + Line

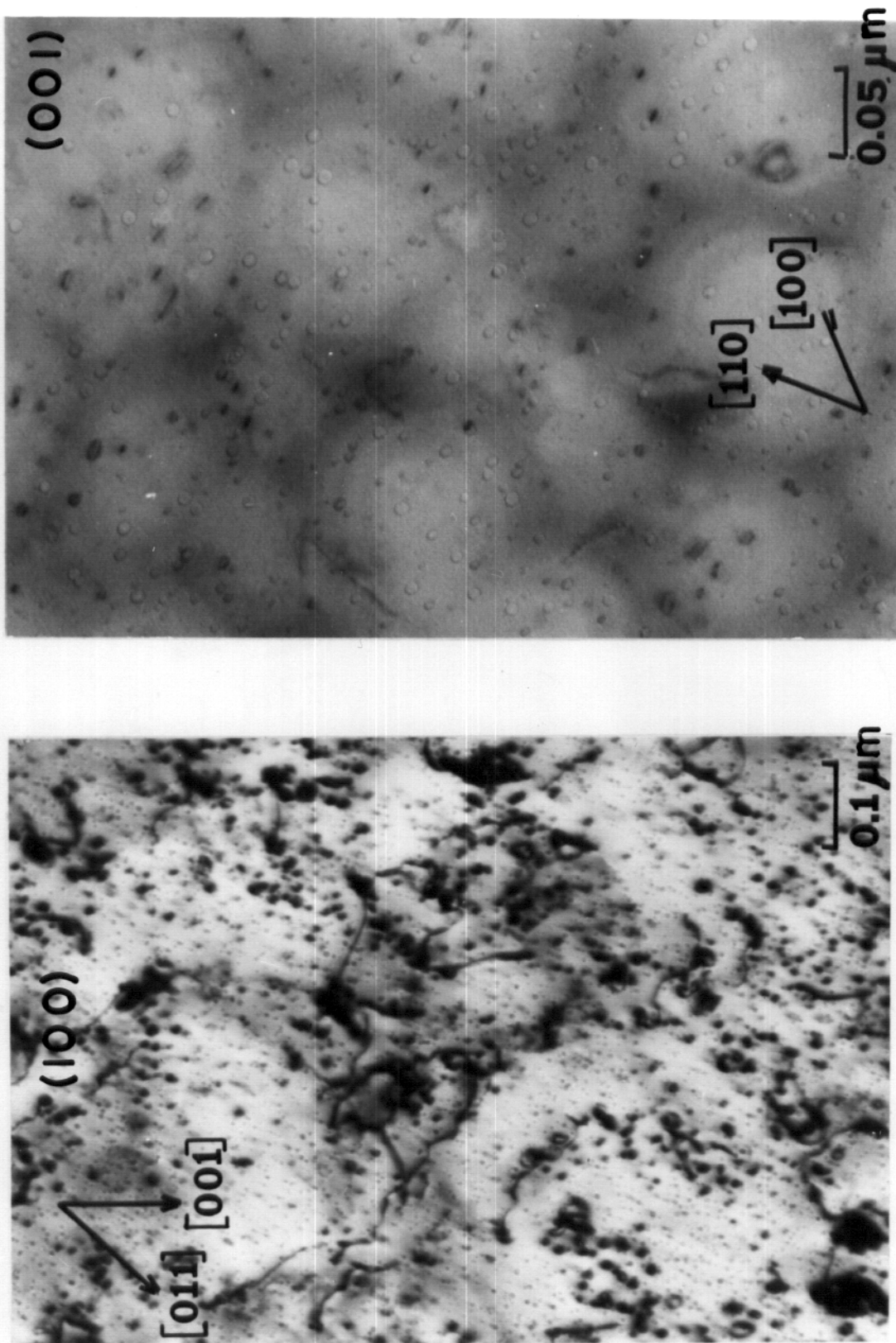


damage microstructures in 5 of the 6 examined specimens are given in Figs. III-V. Figure VI contains histograms of the void size distributions.

The void volume fraction increased as temperature increased from 800°C to 1000°C at the same dpa level (Fig. VII) and at 900°C void swelling increased with increasing dose (Fig. VIII). [Figures VII and VIII are from ref. (4) with corrections made to the UW data for an error in the electron microscope calibration and with estimated errors for the UW data (table IV) added.] However, the average void size at 900°C, 19 dpa was found to be smaller than that at 900°C, 1.9 dpa. The larger void volume fraction at 19 dpa is due to a higher void number density than at 1.9 dpa. A similar decrease in the void diameter with an increase in the void density as dose increased to a certain value in neutron irradiated molybdenum was reported by J. Bentley.<sup>(3)</sup> However, randomly distributed precipitates were observed in the 900°C, 19 dpa specimen. These precipitates could affect the <sup>void</sup> microstructure in this specimen. No precipitates were observed in any other specimen.

Some void depleted zones were observed at grain boundaries with widths varying from 300 Å to 700 Å at 900°C. Figure IX is an electron-micrograph showing the increase in void sizes adjacent to the void depleted zone near a grain boundary. The change in the void size is reduced for narrower depleted zones. This can be explained by differences in the effectiveness of the grain boundaries as defect sinks. The beginning of a void superlattice was observed in the 800°C, 2.2 dpa specimen. A void lattice with better alignment was found in the 900°C, 19 dpa specimen though the alignment was still not perfect as can be seen in Fig. V. The void lattice spacing is about 340 Å in both specimens.

Loop and network dislocation densities were also determined when the foil thickness was determined from stereo pair analysis. The values obtained are given in Table IV. The loop density decreased from  $2 \times 10^{15} \text{ cm}^{-3}$  at 700°C to  $2 \times 10^{13} \text{ cm}^{-3}$



(a)

(b)

Figure IV. Typical microstructures in Mo irradiated to 1.0 dpa at 700°C with 17 MeV copper ions.  
(a) Dislocation structure. (b) Void structure.

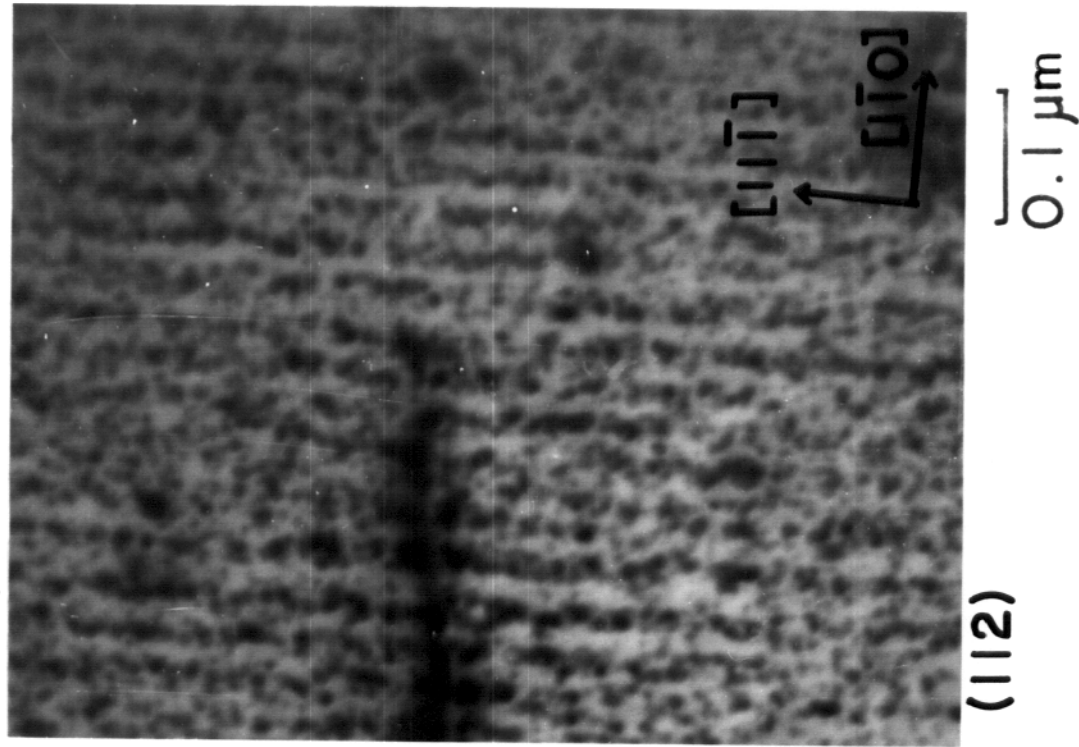
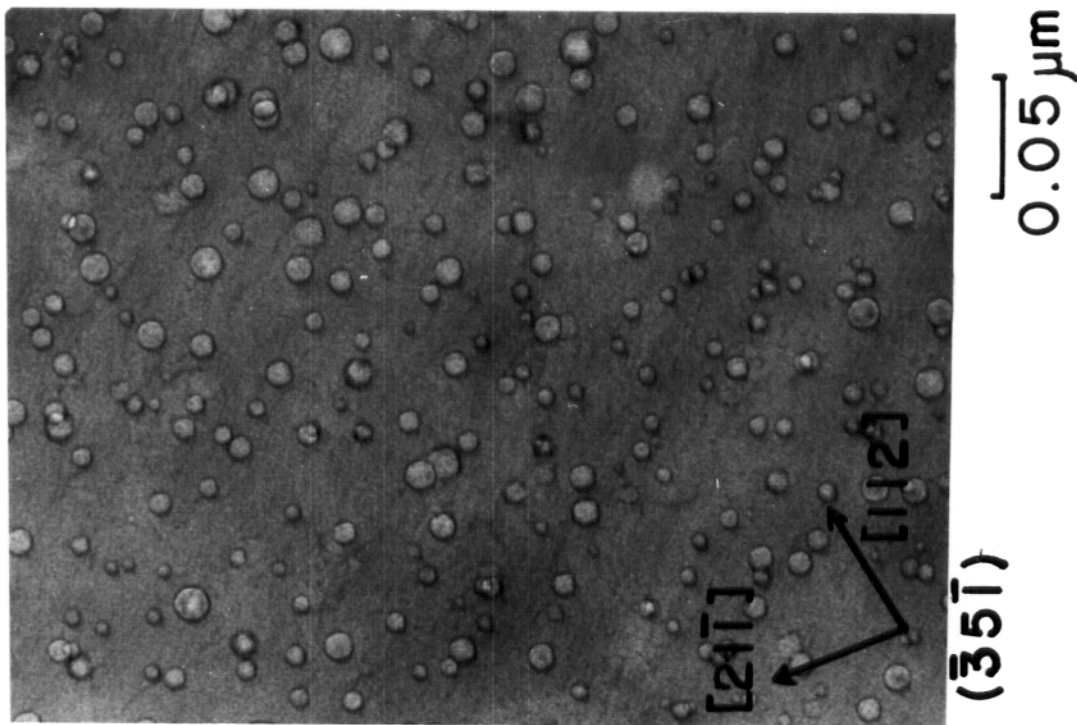


Figure V. Mo irradiated at 900°C to 19 dpa. (a) Void microstructure. (b) Foil orientation chosen to show the void superlattice.

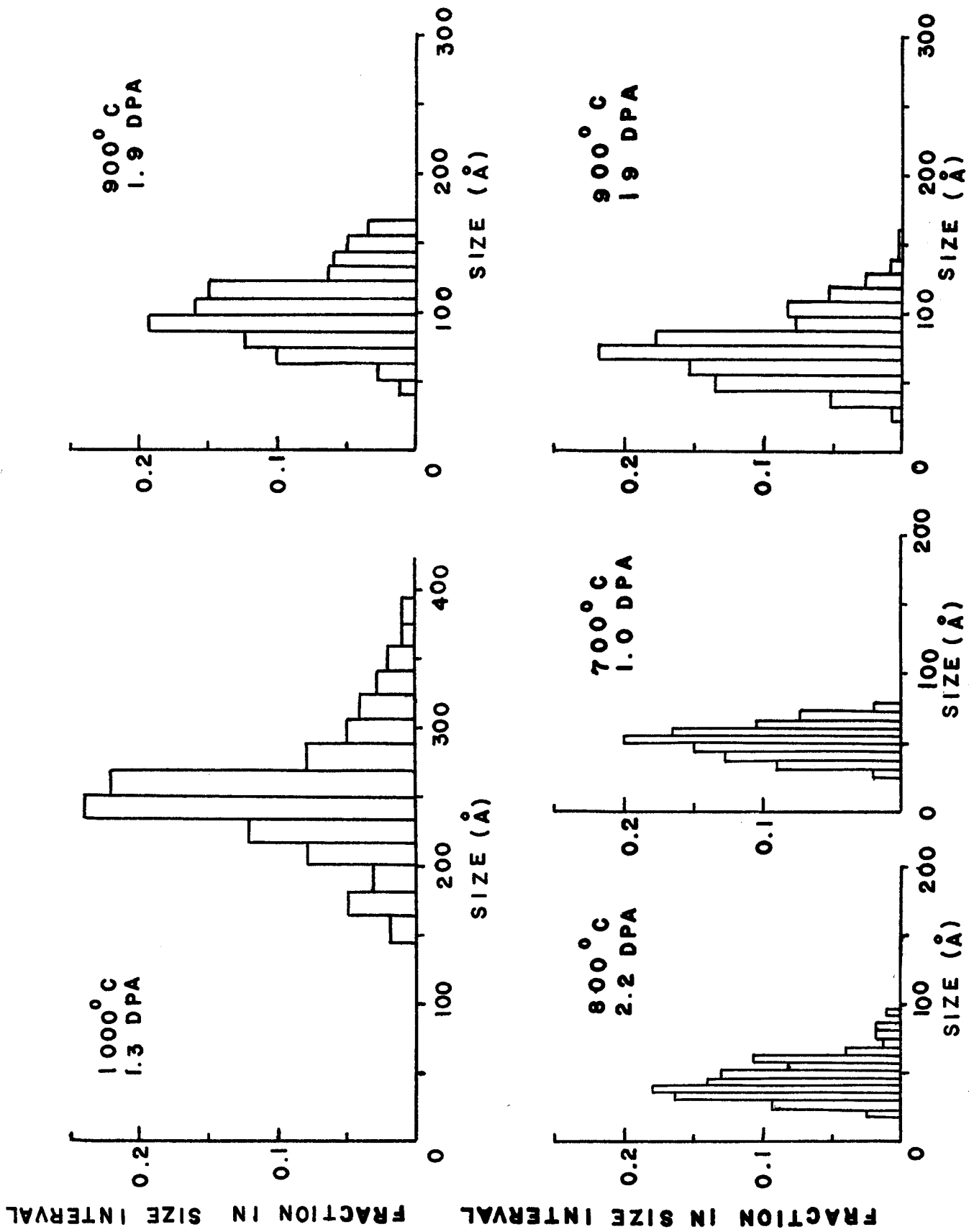


Figure VI. Void size distributions in 5 of the 6 irradiated UW molybdenum specimens.

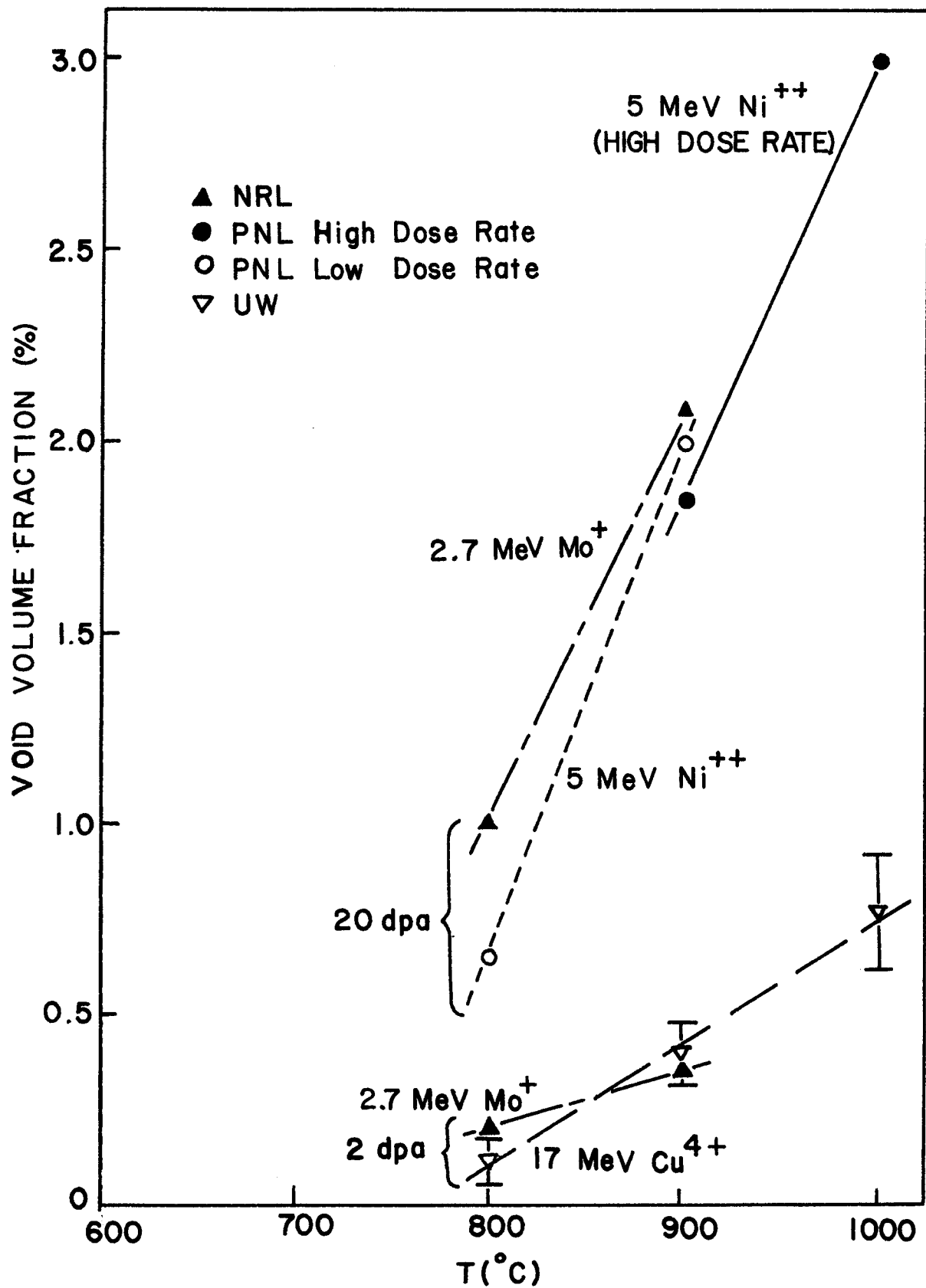


Figure VII. Temperature dependence of swelling in Mo bombarded by different ions. This figure is taken from ref. (4) with corrections made to the UW data for an error in the electron microscope calibration and with the error estimates for the UW data (table IV) added.

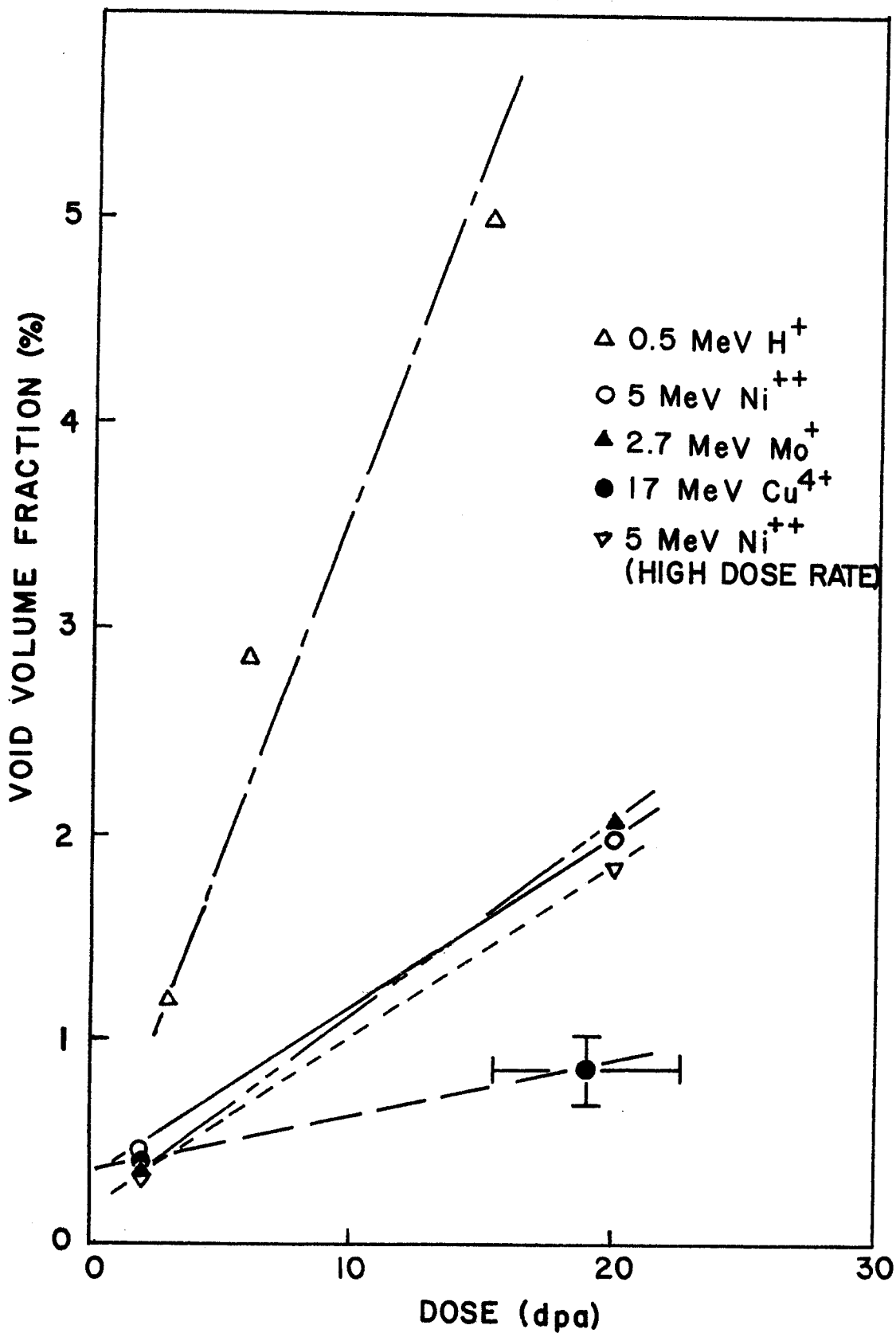


Figure VIII. Dose dependence of swelling in Mo bombarded by different ions at 900°C. This figure is from ref. (4) with corrections made to the UW data for an error in the microscope calibration and with the error estimates for the UW data (table IV) added. For the UW 2 dpa result the error bars are approximately the size of the datum point.



Figure IX. Void denuding near a grain boundary in Mo irradiated at 900°C to 1.9 dpa with 17 MeV copper ions.

at 800°C. At 900°C, loops were observed only in the 19 dpa high dose specimen. No loops were found at 1000°C and 1.3 dpa.

### B. TEM Measurements on the Common Specimen

A TEM specimen supplied by the Naval Research Laboratory was examined by participating sites in the BCC ion correlation program. The same procedure of microscopy analysis and void size measurement as described in section II-B and II-C was applied by one of the authors (KYL) to examine this specimen at U.W. This experiment was designed to obtain the variation in void data due solely to the different microscopy and void size measurement techniques used in different laboratories. The preliminary results of this experiment have been reported by J. L. Brimhall.<sup>(4)</sup>

The University of Wisconsin data together with the averages and standard derivations of data reported by seven participating sites are shown in Table V.

Table V. Common Specimen Results

	Average Void Size (Å)	Void Density (cm <sup>-3</sup> )	Void Volume Fraction (%)
U. W. Data	85 ± 4	6.4x10 <sup>16</sup> ± 1.6x10 <sup>16</sup>	2.6 ± 0.5
Average of Seven Sites	80	7.3 x 10 <sup>16</sup>	2.42
Standard Derivation	7	2.5 x 10 <sup>16</sup>	0.42

Considerable variation was found in the reported void densities due to the uncertainty in measuring the foil thickness and the variation in void sizing and counting techniques. The maximum deviation from the average void volume fraction was ± 25-30 % as reported in reference (4).



### C. Measurement of Void Parameters in the Common Micrograph

Measurements on duplicate copies of a common micrograph supplied by NRL were made by one of us (KYL) using the techniques of counting and sizing voids described in Section II-C. The foil thickness determined by NRL (1050A) for this common micrograph was used to calculate the void volume fraction. The result of this experiment together with the averages and the standard deviations of void parameters determined by eight participating sites<sup>(4)</sup> are shown in table VI.

Table VI. Common Micrograph Results

	<u>Average Void Size</u>	<u>Void Density</u>	<u>Void Volume Fraction</u>
U. W. Data	84 Å	$5.86 \times 10^{16} \text{ cm}^{-3}$	2.2%
Average of Eight Sites	80 Å	$5.84 \times 10^{16} \text{ cm}^{-3}$	2.09%
Standard Deviation	2.3 Å	$0.28 \times 10^{16} \text{ cm}^{-3}$	0.39%

The result of this experiment indicates a  $\pm 20$  % spread in void volume fraction solely due to the variation in the void sizing and counting techniques.

### D. Comparison with Other ICE Ion Simulation Results

In addition to differences in specimen environment at the participating sites, another major variable in the ICE experiment is the energy, type, and resulting dose rate of the ion beams used to induce the damage in the specimens as indicated in table VII.

Table VII. Comparison of Ion Beams Used at the Participating Sites

Site	Ion	Energy (MeV)	Average Dose Rate (dpa/sec)
AI	H <sup>+</sup>	0.5	2 x 10 <sup>-4</sup>
NRL	Mo <sup>+</sup>	2.7	2.5 x 10 <sup>-3</sup>
PNW	Ni <sup>2+</sup>	5	3 x 10 <sup>-3</sup> , 1 x 10 <sup>-2</sup>
UW	Cu <sup>4+</sup>	17,19	4 x 10 <sup>-4</sup>

Figures VII and VIII are from ref. (4) but have been altered to include corrections to the UW data for an error in the electron microscope calibration and to include the error estimates for the UW data given in Table IV. There is reasonable agreement between the UW data and others where there is overlap, except for the 19 dpa, 900° point which does not agree with either the high dose rate Ni<sup>++</sup> and Mo<sup>+</sup> points or the lower dose rate H<sup>+</sup> point. The Ni<sup>++</sup>, Mo<sup>+</sup> and Cu<sup>4+</sup> 2 dpa, 900°C points also do not agree with the H<sup>+</sup> point. This disagreement is probably due to the differences in the PKA spectrum for H<sup>+</sup> and the heavy ions. The 19 dpa, 900°C UW specimen was irradiated at a lower dose rate than the 20 dpa NRL and PNL points, so dose rate effects may also account for the discrepancy. Also, the UW results may have been affected by the low density, uniformly distributed precipitation observed in the 19 dpa specimen.\*

#### IV. Conclusions

1. For molybdenum irradiated to 2 dpa, the peak in the swelling curve is near or above 1000°C.
2. The average void size increases with temperature and the average void density decreases with temperature in the range 700°C to 1000°C at ~ 2 dpa for Mo.
3. The voids formed in molybdenum irradiated to 19 dpa at 900°C form a void lattice with lattice spacing of 34 nm. At 800°C and 2.2 dpa the void lattice is in its initial stages of development with lattice spacing of 34 nm also.

\* This specimen will be examined in the x-ray analysis probe presently being added to the Jeolco electron microscope to attempt to identify the nature and the origin of the precipitates.

4. Dislocation loops were observed only at 700°C and 800°C and not at 900°C or 1000°C at 2 dpa. However, loops were observed in the 900°C, 19 dpa sample.

5. Despite the differences in sample irradiation environment and ion beam species, energy, and dose rate, the void swelling measurements obtained at the University of Wisconsin generally agreed with the measurements obtained at the other sites.

#### Acknowledgements

We express our thanks to the U.W. nuclear physics group for the use of the tandem accelerator to irradiate the specimens. R. G. Lott, W. J. Weber, S. K. McLaurin, J. B. Whitley, and R. Zee assisted with the irradiations and W. J. Weber assisted in development of the electron microscopy techniques. This research was supported in part by a grant from the Division of Physical Research, U. S. Energy Research and Development Administration.

### References

1. H. V. Smith, Jr., and R. G. Lott, Nucl. Instr. Meth. (in press). R. G. Lott and H. V. Smith, Jr., Proc. of Symp. on Experimental Methods for Charged-Particle Irradiations, D. Kramer (ed.), CONF-750947 (September 1975), p. 82.
2. I. Manning and G. P. Mueller, Comp. Phys. Comm. 7, 85 (1974).
3. J. Bentley, "High Temperature Neutron Irradiation Damage in Mo and TZM," Ph.D. Thesis, Univ. of Birmingham, England (1974).
4. J. L. Brimhall, "Summary Report of BCC Ion Correlation Experiment," to be published.